ISSN 1062-8738, Bulletin of the Russian Academy of Sciences: Physics, 2017, Vol. 81, No. 7, pp. 901–906. © Allerton Press, Inc., 2017.
Original Russian Text © M.A. Chuev, 2017, published in Izvestiya Rossiiskoi Akademii Nauk, Seriya Fizicheskaya, 2017, Vol. 81, No. 7, pp. 996–1001.

Excitation Spectrum and Magnetic Dynamics of the Néel Ensemble of Antiferromagnetic Nanoparticles in Mössbauer Spectroscopy

M. A. Chuev

Institute of Physics and Technology, Russian Academy of Sciences, Moscow, 117218 Russia
e-mail: chuev@ftian.ru

Abstract—A continual magnetic dynamics model of an ensemble of antiferromagnetic nanoparticles with uncompensated spin is developed that allows descriptions of the energy spectrum, magnetic dynamics, and Mössbauer spectra of antiferro- and ferromagnetic nanoparticles. Qualitative effects observed experimentally for almost half a century can be explained using this approach, and they can be described quantitatively.

DOI: 10.3103/S106287381707005X

Antiferromagnetic (AFM) nanoparticles are widely used in different fields of engineering, due to the specific structural, magnetic, and thermodynamic properties of such materials. At the same time, the diagnostics of real materials using different experimental methods continues to be based on Néel's phenomenal approach, which describes the superposition of antiferromagnetism and supermagnetism of an uncompensated magnetic moment in two magnetic sublattices [1]. Models allowing the analysis of experimental data have so far been based exclusively on an uncompensated magnetic moment and a simplified interpretation of antiferromagnetism in the context of Néel's linear sucseptibility [2], which inevitably interferes when assessing the derived physical parameters.

Only recently was a way out of this approximation found, along with quantum-mechanical [3] and continual [4] models for describing the thermodynamics and Mössbauer spectra of an ensemble of perfect AFM particles. This immediately allowed qualitative description of the difference between the thermodynamic properties of ferromagnetic (FM) and AFM nanoparticles, particularly the quantum effects observed in the spectra of ^{57}Fe nuclei in the 1960s [5], and specific shapes of the spectra of AFM particles in the macroscopic range [6].

It was also shown that considering uncompensated spin results in no qualitative changes in these effects, but slight numerical corrections in both the quantum model in [7] and the simplified continual model in [8], which is based only on normal modes of the homogeneous precession of magnetization vectors of sublattices (Fig. 1). Even though the homogeneous precession modes are accurate, they are particular solutions of the equation of motion, and their general solution must contain nutations of magnetization against homogeneous precession, in analogy with classic problems on particles in a central field, a spherical pendulum, and a heavy gyroscope [9]. Nutations were considered in the continual model in [4]. However, a quantitative description of experimental data requires generalization of this model for an uncompensated for magnetic moment. The aim of this work was to solve this problem.

In analogy with [4, 8], let us consider the simplest expression for the energy density of AFM particles with exchange interaction constant $J > 0$ and axial magnetic anisotropy constant K in an approximation of two sublattices with magnetization vectors $\vec{M}_1$ and $\vec{M}_2$:

$$E = J\vec{M}_1\vec{M}_2 - \frac{K}{2}\left(\cos^2\theta_1 + \cos^2\theta_2\right), \qquad (1)$$

where θ_1 and θ_2 are the angles between vectors $\vec{M}_1$ and $\vec{M}_2$ and the easy axis. One difference from perfect AFM particles [4] is that the absolute values of M_1 and M_2 can vary in (1). According to the classic theories of AFM [10] and FM [11] resonances, our problem can be considered phenomenologically by assuming that the magnetic moment of each i-th sublattice precesses in the internal effective field:

$$\vec{H}_i^{(\text{eff})} = -\partial E/\partial \vec{M}_i,$$

which satisfies equation of movement

$$\dot{\vec{M}}_i = -\gamma_i\left[\vec{M}_i, \vec{H}_{i-}^{(\text{eff})}\right], \qquad (2)$$

where γ_i is the magnetomechanical relation for the i-th sublattice. In our case, the effective magnetic fields acting on each sublattice are determined by the expressions

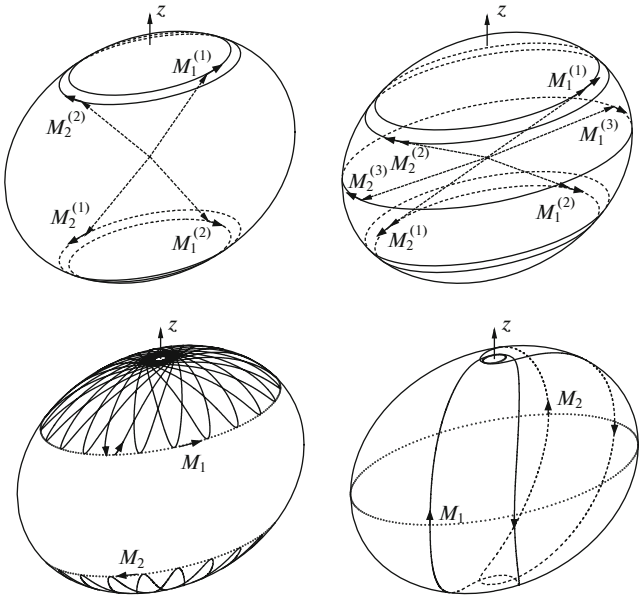

Fig. 1. Trajectory of the motion of sublattice magnetization vectors $\vec{M}_1$ and $\vec{M}_2$ of an ideal AFM particle: (top) normal precession modes with $m_{1,2} = \pm m_{\max}(E)$ and $m_3(E) = \pm 2\sqrt{(1 + E/A)(2 - K/A)}$ for $E/A = -1.003$ (left) and -0.997 (right); (bottom) nutations with $m = 0$ for the same energy values ($A = JM^2$). The points indicate the minimum and maximum values of M_{1z} and M_{2z} projections during nutation. Here and below, the calculations were performed for $K/A = 0.01$.

$$\vec{H}_1^{(\text{eff})} = -H_{E2}\vec{m}_2 + H_{A1}m_{1z}\vec{n}_z,$$

$$\vec{H}_2^{(\text{eff})} = -H_{E1}\vec{m}_1 + H_{A2}m_{2z}\vec{n}_z,$$

where effective exchange field values $H_{Ei} = JM_i$ and anisotropy field $H_{Ai} = K/M_i$ are introduced for each sublattice [10, 11], along with normalized sublattice magnetization values $\vec{m}_i = \vec{M}_i/M_i$ and their projections $m_{iz} = M_{iz}/M_i$ on the easy axis with unit vector $\vec{n}_z$.

The general solutions to equations of motion (2) are described by a set of equations differential with respect to time t for the magnetization components. For longitudinal components of perfect AFM particles in particular, we have [4]

$$dm_{1z} = -dm_{2z} = \pm\omega_E\sqrt{F(m_{1z}, m_{2z}, E)}dt, \qquad (3)$$

where $\omega_E = -\gamma H_E$ and $F(m_{1z}, m_{2z}, E)$ is the quadric polynomial relative to m_{1z} and m_{2z}. According to Eq. (3), along with the energy the integral of motion is the total magnetic moment projected onto the anisotropy axis $m = m_{1z} + m_{2z}$, and Eqs. (3) can be rewritten for longitudinal antiferromagnetism vector component $l_z = m_{1z} - m_{2z}$:

$$dl_z = \frac{\omega_0}{2}\sqrt{\left(l_z^2 - l_1(E,m)\right)\left(l_2(E,m) - l_z^2\right)}dt, \qquad (4)$$

where $\omega_0 = \gamma H_0 \equiv \sqrt{H_A(2H_E + H_A)}$ is the classic AFM resonance frequency in a zero external magnetic field [10]. For fixed E and m values, Eq. (4) determines the time dependence and the range of changes in the longitudinal magnetization components of the sublattices. The latter in turn determine the type and characteristics of the trajectories of the motion of vectors $\vec{M}_1$ and $\vec{M}_2$ in the form of nutations (Fig. 1), i.e., their self-consistent precession around z axis with simultaneous polar angle vibrations in the range given by parameters $l_1(E,m)$ and $l_2(E,m)$ [4, 9]. At the same time, some E and m values satisfy condition $l_1(E,m) = 0$ corresponding to the normal modes of precession (Fig. 1).

According to the generally accepted assumption of the weakness of the energy of anisotropy compared to the energy of exchange, when

$$K \ll A = JM_1M_2,$$

the nutations behave differently in three energy ranges, each of which is characterized by qualitatively different allowed values of m and l_z (Fig. 2). Such a nontrivial profile of the energy excitation spectrum of perfect AFM particles and its effect on physically observed magnitudes were carefully analyzed using the temperature evolution of Mössbauer spectra in [4] as an example. It is worth noting that since the period of high-frequency nutation is much shorter than the characteristic times in most experimental techniques (particularly Mössbauer spectroscopy), the observed characteristics will depend on the average (over the period of nutation) values of $\bar{m}_{1,2z}(E,m)$ components defined by Eq. (4). For perfect AFM particles [4], when $l_1(E,m) > 0$,

$$\bar{m}_{1,2z}(E,m) = \frac{m}{2} \pm \frac{\pi\sqrt{l_2(E,m)}}{4I_1\left(\sqrt{l_1(E,m)/l_2(E,m)}\right)}, \qquad (5)$$

where

$$I_1(\gamma) = \int_\gamma^1 \frac{dx}{\sqrt{\left(x^2 - \gamma^2\right)\left(1 - x^2\right)}},$$

and when $l_1(E,m) < 0$,

$$\bar{m}_{1,2z}(E,m) = m/2. \qquad (6)$$

With an uncompensated magnetic moment in an AFM particle characterized by parameter

$$\beta = \frac{\gamma_2 M_1}{\gamma_1 M_2} < 1,$$

differential Eqs. (3) change slightly:

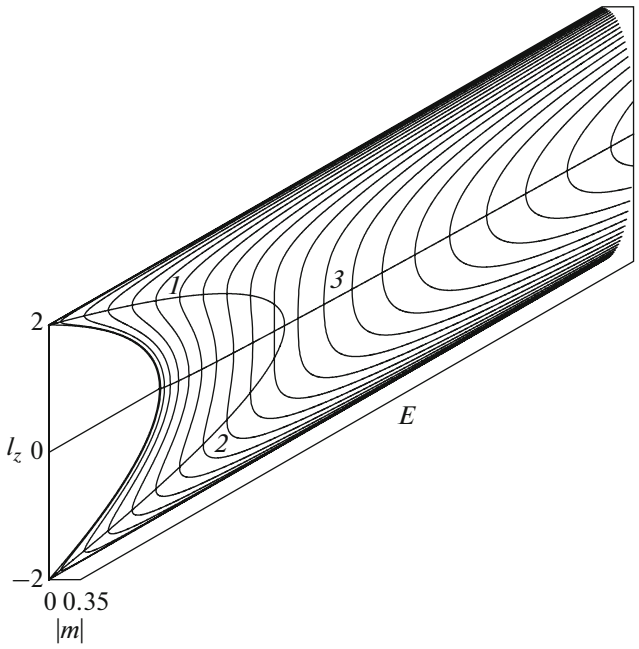

Fig. 2. Allowed values of m and l_z projections for ideal AFM particles. The bold lines with numbers indicate the normal modes of the homogeneous precessions of sublattice magnetic moments with $m = m_{1,2,3}(E)$.

$$\frac{dm_{1z}}{\omega_{E1}} = -\frac{dm_{2z}}{\omega_{E2}} = \pm\sqrt{F(m_{1z}, m_{2z}, E)}dt, \qquad (7)$$

where $\omega_{E1,2} = -H_{E2,1}$, and the integral of motion is also the total magnetic moment projected onto the anisotropy axis $m = \beta m_{1z} + m_{2z}$. However, these equations already have no trivial analytic solutions like those for perfect AFM particles ($\beta = 1$) and the nutation characteristics for the fixed E and m values are found by numerically solving the fourth-order equation

$$F(m_{1z}, m - \beta m_{1z}, E) = 0. \qquad (8)$$

The type and characteristics of the self-consistent trajectories of motion of vectors $\vec{M}_1$ and $\vec{M}_2$ are nevertheless similar in both cases.

Examples of results from such calculations are shown in Fig. 3, where the projection of antiferromagnetic vector $l_z = \beta m_{1z} - m_{2z}$ is introduced for comparison with ideal AFM particles. As we can see, the general solution in the form of three normal modes of the self-consistent precession of vectors $\vec{M}_1$ and $\vec{M}_2$ around an easy axis coated with a layer of nutation is retained even at the uncompensated moment. At low energies, however, the range of allowed m (absolute) values will be limited from below: $|m(E)| \geq m_{\min}(E)$, so only values $m(-A-K) = \pm(1-\beta)$ will be acceptable at the energy minima; at energies above a certain

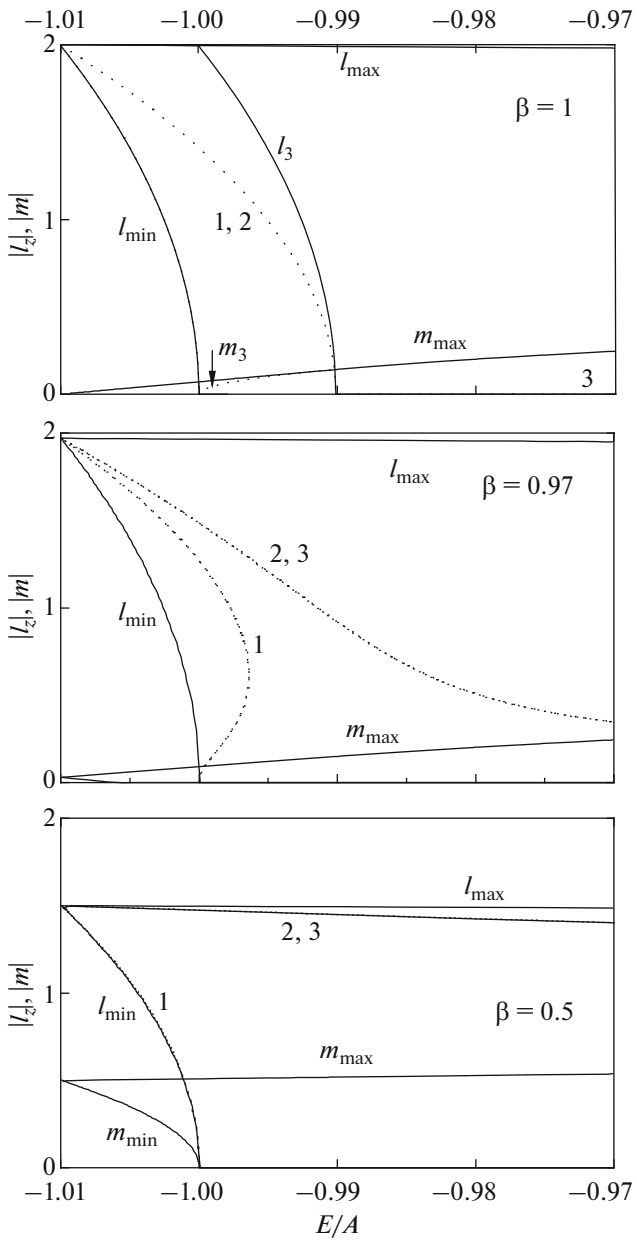

Fig. 3. Allowed values of m and l_z projections for ideal ($\beta = 1$) and uncompensated for AFM particles ($\beta < 1$). The dotted lines correspond to the normal modes of the homogeneous precession of sublattice magnetic moments.

value, $m_{\min}(E) = 0$ is allowed (Fig. 3). The maximum (absolute) $m(E) = \pm m_{\max}(E)$ values are attained for homogeneous precession modes 2 and 3. In analogy with perfect AFM particles [4], the nutation of sublattice magnetization varies in three ranges of energy:

When $E \leq -A$, there are two possible solutions of Eq. (8). The minimum and maximum (absolute) l_z values of the determined energy, and thus the maximum range of nutation around the polar angle, are

observed when $m(E) = \pm m_{\min}(E)$. At the same time, the extreme values of l_z and the range of nutation in the two potential wells corresponding to the two pairs of real roots of Eq. (8) are found to be different, in contrast to perfect AFM particles. However, the symmetry relative to the simultaneous change in the sign of projection m and l_z (or m_{1z}) is retained. The greater the absolute value of m for a given energy, the smaller the range of nutation in both potential wells, attaining $m(E) = \pm m_1(E)$ when homogeneous precession mode 1 is achieved. With a further increase in the (absolute) value of m, the nutations in the potential well corresponding to mode 1 (the two complex roots of Eq. (8)) vanish, and the range of nutation in the other potential well (the two real roots of Eq. (8)) shrinks to $m(E) = \pm m_{\max}(E)$ when homogeneous precession modes 2 and 3 are achieved.

The next range of energies, $-A \le E \le E^{(1)}_{\max}$ ($E^{(1)}_{\max}$ corresponds to the maxim energy for excitation branch 1), in which three modes of homogeneous precession also coexist (Fig. 3), consists of three different ranges according to m. The maximum spread of nutations in both potentialwells (the two real and two complex roots of Eq. (8)) is achieved when $m = 0$. As the absolute value of m for a fixed energy rises, the type of solution remains unchanged until $m(E) = \pm m_{11}(E)$, when mode 1 of homogeneous precession is achieved in the local energy minimum (Fig. 3). With a further increase in the (absolute) value of m, the situation is similar to that in the previous energy range: two ranges of nutation and two pairs of real roots of Eq. (8) up to $m(E) = \pm m_1(E)$, and then one range of nutation (two real and two complex roots of Eq. (8)) until $m(E) = \pm m_{\max}(E)$. Finally, in the third energy range $E \ge E^{(1)}_{\max}$, all possible values of m at a fixed energy result in two real and two complex roots of Eq. (8), while nutations spread in both potential wells up to $m(E) = \pm m_{\max}(E)$, when modes 2 and 3 of homogeneous magnetization precession are achieved.

As for calculating the longitudinal magnetization components of the sublattices, their average (over the range of nutation) values for fixed E and m can be calculated via the common transformation of the integral presented by Eq. (7) to the canonic form of a first-degree elliptic integral by introducing quadric polynomial $F(m_{1z}, m - \beta m_{1z}, E)$ with known roots $m^{(i)}_{1z}$ ($i = 1$, 2, 3, 4) to the product of binomials with respect to m^2_{1z}.

The Mössbauer spectra of an ensemble of randomly oriented AFM particles in the simplest limiting case of slow (compared to the frequency of precession and the reverse lifetime of an exited nucleus) sublattice magnetization relaxation can be calculated using the results reported in [4, 8], generalized for an uncompensated for spin. The equilibrium state of the ensemble of particles at fixed temperature T is thus described by a Gibbs distribution with respect to quasi-stationary states (the precession and nutation orbits of vectors $\vec{M}_1$ and $\vec{M}_2$) with fixed E and $m(E)$ values), each of which is characterized by the average values of the longitudinal magnetization components of sublattices $\bar{m}_{1z}(E,m)$ and $\bar{m}_{2z}(E,m) = m - \beta\bar{m}_{1z}(E,m)$:

$$W(E,m) = Ce^{-EV/k_BT}, \qquad (9)$$

where V is the particle volume and C is the normalizing constant. The cross-section of the absorption of gamma-quanta with energy $E_\gamma = \hbar\omega$ when there is no hyperfine quadrupole interaction is defined as

$$\sigma(\omega) = \frac{\sigma_a}{2}\int dE W(E) \int\limits_{m(E)} dm \sum_{i=1}^{2}\sum_{j}\left|L\left(\omega, \bar{m}^{(j)}_{iz}(E,m)\right) + L\left(\omega, \bar{m}^{(j)}_{iz}(E,-m)\right)\right|, \qquad (10)$$

where the partial absorption spectra corresponding to quasi-stationary states are determined by Lorenzians $L(\omega, x)$ [4, 8].

For a Néel ensemble of slowly relaxing AFM particles, we must also average over the random value of uncompensated for spin, e.g., with respect to the Gauss distribution of parameter β with average value $\bar{\beta} = 0$ and width σ_β. The typical absorption spectra of ensembles of slowly relaxing ideal ($\beta = 1$) and Néel ($\bar{\beta} = 1, \sigma_\beta = 0.03$) AFM nanoparticles are presented in Fig. 4. Calculations do reveal the above features of the energy spectrum of AFM particles and their emergence in the absorption spectra: a transition from a well-resolved magnetic superthin structure at low temperatures to a high-temperature single line against a magnetic hyperfine structure with strikingly asymmetric lines at intermediate temperatures and a high-temperature single line in accordance with quantum-mechanical calculations on the macroscopic scale [3, 7]. Our calculations confirm yet another important conclusion following from the quantum model: the presence of an uncompensated spin in the slow relaxation regime does not change the qualitative behavior of the spectrum shapes of ideal AFM particles as the temperature varies, but results in only slight quantitative corrections in the central part of the spectrum that are obvious at high temperatures. Additional consideration of sublattice magnetization nutations evens out this difference compared to the data from [8], where only homogeneous precession modes were taken into account.

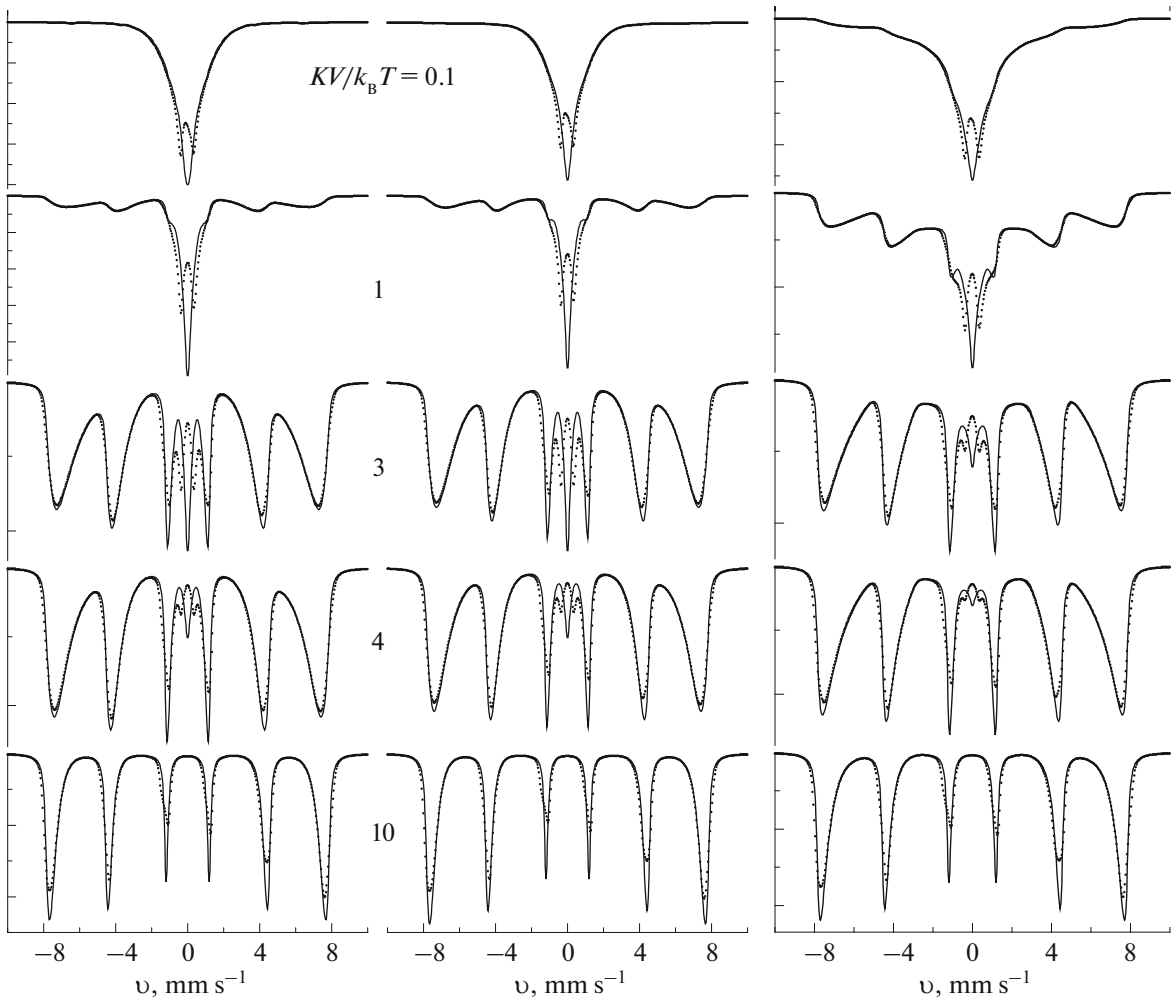

Fig. 4. Mössbauer absorption spectra of ^{57}Fe nuclei in an ensemble of ideal ($\beta = 1$) AFM particles (left), AFM particles with a Gaussian distribution ($\bar{\beta} = 1$ and $\sigma_\beta = 0.03$) of an uncompensated magnetic moment (center) and ferromagnetic particles with $\beta = 0.5$ (right). The calculations were performed within the limits of slow relaxation for different values of effective energy barrier KV/k_BT in the presence of quadrupole interaction with constant q (points) and its absence ($q = 0$, solid lines): $q = 0.35$ mm s^{-1} and $H_{hf} = 500$ kOe.

The normal precession modes of vectors $\vec{M}_1$ and $\vec{M}_2$, the excitation branches in the energy spectrum, and the allowed values for sublattice magnetization nutations of AFM particles with $\beta = 0.5$ shown in the bottom panel of Fig. 3, formally correspond to ferromagnetic particles. Such precession modes correspond to classic FM resonance theory [11], which is characterized by the low- and high-frequency precession of sublattice magnetizations. Normal mode 1 in Fig. 3 can be attributed to the low-frequency self-consistent precession of oppositely directed vectors $\vec{M}_1$ and $\vec{M}_2$, while normal modes 2 and 3 belong to the high-frequency precession of these vectors at different angles to the anisotropy axis.

The absorption spectra calculated for $\beta = 0.5$ are displayed in the right column of Fig. 4, and are comparable to the spectra simulated in the simplified model in [8]. The difference between the partial spectra for the two magnetic sublattices grows monotonically at slow relaxation as the temperature rises, and both the resulting spectrum and the two partial spectra reveal a specific magnetic hyperfine structure with lines of quasi-triangular shape against the distorted five-step base at high temperatures. This profile of absorption spectra is evidently due to partial contributions from excitation branches 1, 2, 3 in the energy spectrum for the corresponding homogeneous precession modes and their appropriate nutations for $\beta = 0.5$ (Fig. 3). These spectral shapes have often been observed in experiments (see Refs. in [12]).

CONCLUSIONS

A formalism for describing the thermo- and magnetic dynamics of a Néel ensemble of AFM particles with an uncompensated magnetic moment was elaborated in a generalized continual magnetic dynamics model for an ensemble of ideal AFM particles in a two-sublattice approximation. This enabled us to develop a theory of Mössbauer absorption spectra for such materials that can be applied in the analysis of experimental spectra. Calculations within the proposed macroscopic model confirm the basic conclusions of the quantum-mechanical model developed in [3, 7] for an ensemble of AFM particles.

ACKNOWLEDGMENTS

This work was supported by the Russian Foundation for Basic Research.

REFERENCES

1. Néel, L., *C. R. Hebd. Seances Acad. Sci.*, 1961, vol. 252, p. 4075.
2. Silva, N.J.O., Millan, A., Palacio, F., et al., *Phys. Rev. B*, 2009, vol. 79, p. 104405.
3. Chuev, M.A., *JETP Lett.*, 2012, vol. 95, no. 6, p. 295.
4. Chuev, M.A., *JETP Lett.*, 2016, vol. 103, no. 3, p. 175.
5. Kündig, W., Bömmel, H., Constabaris, G., and Lindquist, R.H., *Phys. Rev.*, 1966, vol. 142, p. 327.
6. Mischenko, I.N. and Chuev, M.A., *Hyperfine Interact.*, 2016, vol. 237, p. 21.
7. Chuev, M.A., *Dokl. Phys.*, 2012, vol. 57, no. 11, p. 421.
8. Chuev, M.A., *Bull. Russ. Acad. Sci.: Phys.*, 2015, vol. 79, no. 8, p. 955.
9. Landau, L.D. and Lifshitz, E.M., *Mekhanika* (Mechanics), Moscow: Nauka, 1988.
10. Kittel, C., *Phys. Rev.*, 1951, vol. 82, p. 565.
11. Wangsness, R.K., *Phys. Rev.*, 1953, vol. 91, p. 1085.
12. Chuev, M.A. and Hesse, J., in *Magnetic Properties of Solids*, Tamayo, K.B., Ed., New York: Nova Sci. Publ., 2009, pp. 1–104.

Translated by O.A. Maslova